Determination of Complex Permittivity of Low-Loss Dielectrics

Robert H. Voelker, *Senior Member, IEEE*, Guang-Tsai Lei, *Member, IEEE*, Guang-Wen Pan, *Senior Member, IEEE*, and Barry K. Gilbert, *Senior Member, IEEE*

***Abstract*— A new high-order-mode analytical method is described for calculating the frequency-dependent complex permittivity of a low-loss dielectric in a parallel-plate structure using a planar microwave circuit model. An analytical expression for the complex permittivity is derived in terms of the terminal impedance at a modal resonant frequency of the structure. The derivation provides physical and mathematical insight into the relation between complex permittivity and port impedance. The technique is validated by good agreement between manufacturer's specifications and complex permittivity calculated from measurements near resonant frequencies for a printed circuit board (PCB).**

***Index Terms*—Dielectric losses, dielectric measurements, high-speed circuits/devices, microwave circuits, microwave measurements, microwave resonators, multichip modules, printed circuits.**

I. Introduction

THE complex permittivity of a dielectric material used in high-speed and microwave circuits determines important characteristics such as impedance, phase velocity, and attenuation in signal transmission structures. The electrical performance of a printed circuit board (PCB) or multichip module (MCM) can be significantly influenced by the dielectric properties of the substrate material. For example, the reduction in power and ground plane noise in a PCB or MCM is strongly affected by the complex permittivity of the dielectric material [1]. Thus, it is important to accurately determine the complex permittivity for correct modeling and simulation of these systems.

Extensive research has been performed on determination of material complex permittivity during the last three decades (e.g., the cavity resonance method, conductor method, and waveguide-aperture method [2]–[11]). These methods are often complicated, especially when accurate results are required. A simple and practical method for calculating the dielectric constant and loss tangent of thin dielectric films embedded in a parallel-plate capacitor was developed based on the measured admittance of a capacitor [12], [13]. At microwave frequencies, the admittance at the terminals of a parallel-plate structure such as a two-metal-layer PCB or MCM can be calculated from the scattering parameter S_{11}, measured using a network analyzer. With this approach, the loss tangent $\tan\delta$ is simply calculated as the ratio of the real part to imaginary part of the port admittance of the structure, while the dielectric constant is determined from the imaginary part of the port admittance and the geometrical dimensions of the structure. For measurement frequencies where the stored electric energy dominates the stored magnetic energy—far below the capacitor's first resonant frequency—this method provides a good estimate of dielectric constant and loss tangent, since the dielectric loss tangent of a material is proportional to the ratio of the density of energy dissipated in the material to the stored electric-energy density [14].

At low frequencies, the contributions to the energy dissipation and energy storage from the resistive and reactive elements are decoupled [15]. In contrast, at high frequencies where the plate size is no longer small compared to the wavelength of the signals, the stored electromagnetic energy contributes partially to the resistance, and the power dissipation contributes partially to the reactance. At high frequencies, the total reactance of the parallel-plate capacitor depends on the multiple modes of the full-wave equivalent circuit of the structure, and as the frequency increases, it alternately becomes inductive, then capacitive, and so on [1]. This behavior is controlled by the separation and size of the plates, the location and size of the terminals (ports) on the plates, and the properties of the dielectric [16]. At resonant frequencies, the imaginary part of the port impedance is zero, and thus the ratio of the real part to imaginary part of the port impedance becomes infinite. The previously described complex permittivity calculation technique based on port admittance would yield zero dielectric constant and infinite loss tangent, and thus should not be used near the resonant frequencies.

This paper focuses on a new high-order-mode method for evaluating the complex permittivity of a film dielectric in a parallel-plate structure. This technique has wide applicability in material electrical property measurements, since thin film samples can be produced from many materials. We will derive equations for the complex permittivity of a parallel-plate structure in terms of the modal impedance. These equations will then be shown to collapse into the above-mentioned

Manuscript received January 8, 1997; revised May 23, 1997. This work was supported in part by DARPA/ESTO under Contract N66001-89-C-0104 and Contract N66001-94-C-0051 from NCCOSC/NRaD.

R. H. Voelker is with Sun Microelectronics Division, Sun Microsystems, Inc., Palo Alto, CA 94303 USA.

G.-T. Lei and B. K. Gilbert are with the Department of Physiology and Biophysics, Mayo Foundation, Rochester, MN 55905 USA.

G.-W. Pan is with the Department of Electric Engineering, Arizona State University, Tempe, AZ 85287-7206 USA.

Publisher Item Identifier S 0018-9480(97)07386-9.

approximations for complex permittivity at low frequencies. The low-frequency approximations will be shown to be in error at high frequencies for a PCB example. In contrast, the high-order-mode complex permittivity calculation technique will be shown to give good results near the modal resonant frequencies for this structure. The effect of loss in the conducting planes will also be studied.

II. Derivation and Discussion of High-Order-Mode Equations for Complex Permittivity

Based on the model for port impedance for a planar microwave circuit [17] and for the two-metal-layer power-ground plane structure [16], we have developed closed-form equations to calculate the complex permittivity at the modal resonant frequencies. First, we assume that the two metal planes are perfectly conducting. According to [16, eq. (4)], the mnth modal impedance of the structure Z_{mn} can be written as

$$Z_{mn} = \frac{2k_r k_i}{\left[\left(k_{xm}^2 + k_{yn}^2\right) - \left(k_r^2 - k_i^2\right)\right]^2 + 4k_r^2 k_i^2}\omega H + j\frac{\left(k_{xm}^2 + k_{yn}^2\right) - \left(k_r^2 - k_i^2\right)}{\left[\left(k_{xm}^2 + k_{yn}^2\right) - \left(k_r^2 - k_i^2\right)\right]^2 + 4k_r^2 k_i^2}\omega H \quad (1)$$

where $j = \sqrt{-1}$, $k \equiv k_r - jk_i = \omega\sqrt{\mu\epsilon}$ is the wavenumber with ω being angular frequency, $k_{xm} = m\pi/P_x$, and $k_{yn} = n\pi/P_y$, with m representing the mth eigenmode in the x-direction and n representing the nth eigenmode in the y-direction, and P_x and P_y are the widths of the perfectly conducting plates in the x- and y-directions, respectively (see Fig. 1). To compensate for the field fringing along the periphery of the structure, the physical widths of the planes in the x- and y-directions are converted into equivalent electrical widths by [17, eq. (2.75)] and these are used instead for the widths P_x and P_y in (1). The dielectric has complex permittivity $\epsilon \equiv \epsilon_r - j\epsilon_i$ and permeability μ. Coefficient H is

$$H \equiv \frac{\mu d C_m^2 C_n^2}{P_x P_y}\cos(k_{yn}T_y)^2 \cos(k_{xm}T_x)^2 \times \left[\frac{\sin\left(k_{yn}\frac{L_y}{2}\right)}{k_{yn}\frac{L_y}{2}}\right]^2 \left[\frac{\sin\left(k_{xm}\frac{L_x}{2}\right)}{k_{xm}\frac{L_x}{2}}\right]^2 \quad (2)$$

where L_x and L_y are the port widths in the x- and y-directions, respectively, T_x and T_y represent the location of the center of the port in the x- and y-directions, respectively, and d is the dielectric thickness between the parallel plates. Coefficient $C_m = 1$ if $m = 0$, and $C_m = \sqrt{2}$ otherwise. Similarly, $C_n = 1$ if $n = 0$, and $C_n = \sqrt{2}$ otherwise. Equation (1) is valid for signal wavelengths much larger than d. Equation (1) is represented by a parallel conductance–inductance–capacitance circuit, except for the $m = 0$, $n = 0$ mode, for which it is represented by a parallel conductance–capacitance circuit [16]. The total port impedance of the parallel-plate capacitor is the double summation over m and n of all modal impedances Z_{mn}, and is represented by a series connection of all the modal parallel circuits. Each parallel circuit has a modal resonant frequency at which its reactance is zero. Likewise, the series combination of the parallel circuits has a system resonant frequency at which the total reactance is zero.

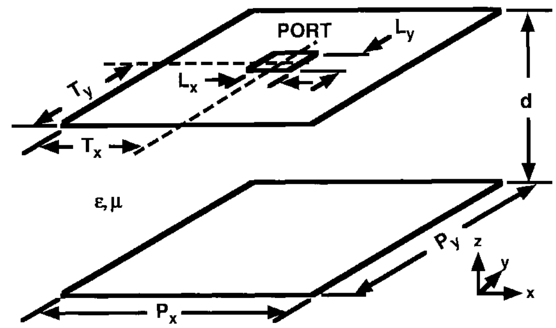

Fig. 1. Parallel-plate capacitor structure [17].

Letting $f_1 \equiv (k_{xm}^2 + k_{yn}^2) - (k_r^2 - k_i^2)$ and $f_2 \equiv 2k_r k_i$ allows the real and imaginary parts of the mnth modal impedance Z_{mn} to be written, respectively, as

$$Z_{mn}^r = \frac{2k_r k_i}{\left[\left(k_{xm}^2 + k_{yn}^2\right) - \left(k_r^2 - k_i^2\right)\right]^2 + 4k_r^2 k_i^2}\omega H = \frac{f_2 \omega H}{f_1^2 + f_2^2} \quad (3)$$

$$Z_{mn}^i = \frac{\left(k_{xm}^2 + k_{yn}^2\right) - \left(k_r^2 - k_i^2\right)}{\left[\left(k_{xm}^2 + k_{yn}^2\right) - \left(k_r^2 - k_i^2\right)\right]^2 + 4k_r^2 k_i^2}\omega H = \frac{f_1 \omega H}{f_1^2 + f_2^2}. \quad (4)$$

Dividing (3) by (4) yields

$$\frac{f_2}{f_1} = \frac{Z_{mn}^r}{Z_{mn}^i} \quad (5)$$

and adding (3) and (4) gives

$$Z_{mn}^r + Z_{mn}^i = \frac{\left(\frac{Z_{mn}^i}{Z_{mn}^r} + 1\right)\omega}{\left[\left(\frac{Z_{mn}^i}{Z_{mn}^r}\right)^2 + 1\right] f_2} H. \quad (6)$$

Thus, f_1 and f_2 can be expressed as

$$f_1 = \frac{Z_{mn}^i}{{Z_{mn}^r}^2 + {Z_{mn}^i}^2}\omega H \quad (7)$$

$$f_2 = \frac{Z_{mn}^r}{{Z_{mn}^r}^2 + {Z_{mn}^i}^2}\omega H. \quad (8)$$

Since $\epsilon \equiv \epsilon_r - j\epsilon_i$, then

$$k^2 = \mu\epsilon\omega^2 = \mu\omega^2\epsilon_r - j\mu\omega^2\epsilon_i \quad (9)$$

and also

$$k^2 = (k_r - jk_i)^2 = \left(k_r^2 - k_i^2\right) - j2k_r k_i. \quad (10)$$

Since ϵ_r and ϵ_i are even and odd functions of frequency, respectively, [18], [19], and ϵ_i is positive except at zero frequency, it follows that k_r and k_i are also even and odd functions of frequency, respectively.

Solving (9) and (10) for the real and imaginary parts of ϵ, and substituting (7) and (8), the explicit formulas relating

Z^r_{mn} and Z^i_{mn} to ϵ_r and ϵ_i are

$$\begin{aligned}\epsilon_r &= \frac{\left(k_r^2 - k_i^2\right)}{\mu\omega^2} = \frac{k_{xm}^2 + k_{yn}^2 - f_1}{\mu\omega^2} \\ &= \frac{\left(k_{xm}^2 + k_{yn}^2\right)\left({Z^r_{mn}}^2 + {Z^i_{mn}}^2\right) - Z^i_{mn}\omega H}{\mu\omega^2\left({Z^r_{mn}}^2 + {Z^i_{mn}}^2\right)} \\ &= \frac{\left(k_{xm}^2 + k_{yn}^2\right)}{\mu\omega^2} - \frac{Z^i_{mn} H}{\mu\omega\left({Z^r_{mn}}^2 + {Z^i_{mn}}^2\right)} \end{aligned} \tag{11}$$

$$\epsilon_i = \frac{2k_r k_i}{\mu\omega^2} = \frac{f_2}{\mu\omega^2} = \frac{Z^r_{mn} H}{\mu\omega\left({Z^r_{mn}}^2 + {Z^i_{mn}}^2\right)} \tag{12}$$

$$\tan\delta \equiv \frac{\epsilon_i}{\epsilon_r} = \frac{Z^r_{mn}\omega H}{\left(k_{xm}^2 + k_{yn}^2\right)\left({Z^r_{mn}}^2 + {Z^i_{mn}}^2\right) - Z^i_{mn}\omega H}. \tag{13}$$

Equations (12) and (13) are valid provided that the metal plates have infinite conductivity.

For the static $(m = 0,\ n = 0)$ case, only the first mode contributes to the impedance, so $Z = Z_{00}$, and the factor $(k_{xm}^2 + k_{yn}^2)$ is zero. Thus, (13) reduces to $\tan\delta = -Z^r/Z^i$, equivalent to [12, eq. (1)], and (11) reduces to

$$\epsilon_r = \frac{-Z^i H}{\mu\omega({Z^r}^2 + {Z^i}^2)}. \tag{14}$$

For $Z^r \ll Z^i$, (14) becomes equivalent to [12, eq. (2)].

At the mnth modal resonant frequency, $Z^i_{mn} = 0$ and Z^r_{mn} is maximum, so (11) yields

$$\epsilon_r = \frac{k_{xm}^2 + k_{yn}^2}{\mu\omega^2} \tag{15}$$

and (12) gives

$$\epsilon_i = \frac{H}{\mu\omega Z^r_{mn}}. \tag{16}$$

Thus, ϵ_r now becomes a simple function of mode numbers and angular resonant frequency, and ϵ_i is related to the real part of the modal impedance.

III. Simulation of a PCB Using High-Order-Mode Complex Permittivity Equations

To utilize only one modal impedance in the determination of the complex permittivity, it must dominate the system impedance $(Z \approx Z_{mn})$. Because of the near singular property of the real and imaginary parts of Z_{mn} at the modal resonant frequency, Z_{mn} does dominate Z. We will utilize the single-mode dominance by considering frequencies at the modal resonances while employing (11) and (13) to calculate the complex permittivity.

As stated in Section I, when the operating frequency is far below the first system resonant frequency of the parallel-plate structure, the capacitive behavior dominates the total reactance, and the resistive and reactive effects are decoupled. Under this condition, the loss tangent can be approximated by $\tan\delta \approx -Z^r/Z^i$. As the frequency increases, the ratio of stored magnetic energy to stored electric energy increases, causing the accuracy of the estimated loss tangent and dielectric constant to worsen. For example, consider the 16.51×16.51 cm^2 double-sided PCB with copper power and ground planes, as shown in Fig. 1 and discussed in [16]. The copper planes are 17.78-μm thick and are separated by a dielectric layer 1.524-mm thick with relative permittivity $\epsilon_r/\epsilon_o = 4.2$, where ϵ_o is the permittivity of free space, and loss tangent of 0.01 up to the gigahertz frequency range. Since the terminals (ports) of size 0.333×0.333 mm^2 are geometrically centered on the planes, the fundamental modal resonance at 440 MHz is suppressed and the first observable resonance occurs at 883 MHz and the second one at 1.25 GHz. The impedance is calculated from (1) by double-summing over m and n all contributions of modes $m = 0, \cdots, m_{\text{MAX}}$, $n = 0, \cdots, n_{\text{MAX}}$, where $m_{\text{MAX}} = n_{\text{MAX}} = 199$. Table I summarizes the dielectric constant and loss tangent calculated from the approximate formulas discussed in Section I. As the frequency increases, the percentage errors between the calculated and actual dielectric constant and loss tangent significantly increase, and thus the high-order-mode technique should be used instead at high frequencies.

TABLE I
Dielectric Constant and Loss Tangent and Their Errors Calculated from the Impedance Using a Simple Static Approximation at Frequencies Below the First System Resonance

Freq. (MHz)	ϵ_r/ϵ_o	ϵ_r/ϵ_o Error (%)	$\tan\delta$	$\tan\delta$ Error (%)
10	4.32	0.4	0.010	0.4
30	4.44	3.3	0.010	3.9
50	4.72	9.7	0.011	9.7
60	4.93	14.6	0.012	14.6
70	5.21	21.0	0.012	21.1
80	5.56	29.4	0.013	29.4
90	6.04	40.4	0.014	40.5
100	6.67	55.1	0.016	55.2
110	7.54	75.5	0.018	75.7

In calculating complex permittivity using the high-order-mode technique, we will utilize the dominance of a modal impedance on the total port impedance at the modal resonant frequency. To demonstrate the dominance of a modal impedance near its resonant frequency on the total impedance of the structure, the $m = 0,\ n = 2$ and $m = 2,\ n = 0$ modes, which are at the same frequency, and the double-summation of the first $m_{\text{MAX}} = n_{\text{MAX}} = 199$ modal impedances are plotted over the frequency range between 100 MHz and 1.5 GHz in Fig. 2. The curve for the summed 200×200 modal reactance is always above that of the single modal reactance at frequencies below the first modal resonance, which is at 0.883 GHz in this case. For frequencies approaching this resonance, the discrepancy between the two curves decreases and nearly vanishes at frequencies close to the resonance. The discrepancy is much more frequency-sensitive for the reactance than for the resistance. Near the

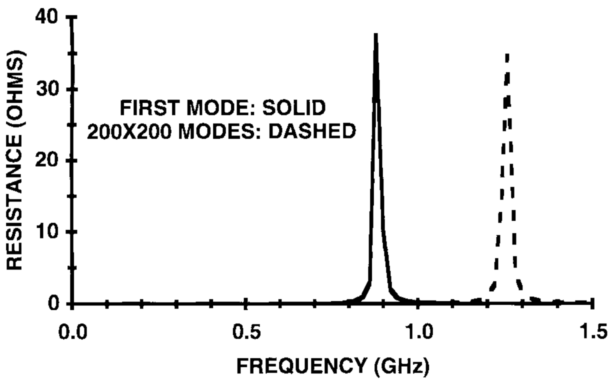

(a)

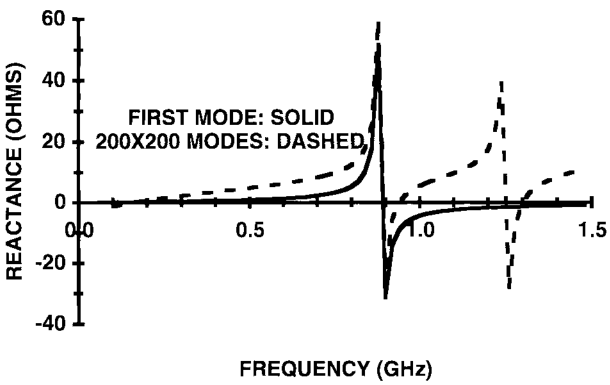

(b)

Fig. 2. Comparison of single mode and total impedances based on the two-dimensional microwave planar circuit model. (a) Resistance. (b) Reactance.

TABLE II
DIELECTRIC CONSTANT AND LOSS TANGENT CALCULATED FROM IMPEDANCE NEAR MODAL RESONANT FREQUENCIES OF THE PCB

Freq. (GHz)	0.8832	0.8830	0.8800	0.8700
Z^r (Ω)	53.760	53.835	36.516	5.405
Z^i (Ω)	1.158	3.595	28.350	19.315
ϵ_r/ϵ_o	4.2261	4.2262	4.2276	4.2454
Rel. Error (ϵ_r/ϵ_o) (%)	0.5	0.5	0.7	1.1
$\tan\delta$	.0100	.0100	.0092	.0073
Rel. Error ($\tan\delta$) (%)	0.0	0.0	8	27

first modal resonance, the resistances of the first mode and of the 200 $\times$ 200 modes are indistinguishable in Fig. 2, while the difference between the reactance for the two cases varies considerably with frequency. At the next resonance of 1.25 GHz, the impedance contribution of the first mode is clearly small compared to the 200 $\times$ 200 modal impedance. Thus, $Z \approx Z_{mn}$ is a good approximation if the operating frequency is selected close to the resonant frequency of mode m, n.

As an example of applying (11) and (13) to calculation of the dielectric constant and loss tangent from the impedance near modal resonances of a parallel-plate structure, we select

TABLE III
DIELECTRIC CONSTANT, LOSS TANGENT, AND THEIR RELATIVE ERRORS CALCULATED FROM IMPEDANCE AT THREE DIFFERENT FREQUENCIES NEAR THE THEORETICAL (2, 2) MODAL RESONANCE (1.2493 GHz) OF THE PCB

Freq. (GHz)	1.2494	1.2487	1.2400	1.2300
Z^r (Ω)	75.467	76.160	25.330	7.420
Z^i (Ω)	0.520	7.930	42.500	29.030
ϵ_r/ϵ_o	4.2243	4.2250	4.2326	4.2532
Rel. Error (ϵ_r/ϵ_o) (%)	0.6	0.6	.8	1.3
$\tan\delta$	.0101	.0099	.0079	.0064
Rel. Error ($\tan\delta$) (%)	1.0	1.0	21	36

the input port at the center of the power-ground plane structure. Thus, all modes with at least one index—m or n—being an odd number are suppressed due to the cosine factors involved in the coefficient H, and the peaks of the evenly numbered model impedances will be clearly distinguished in the frequency domain. For the square board, the first nonzero modes (0, 2) and (2, 0) have an identical modal impedance, thus the input impedance $Z_{\rm in}$ calculated as a sum of the two dominate modal impedances at the first degenerate resonance can be divided by two to obtain a single modal input impedance for either mode. Following the procedure, first we calculate the theoretical resonant frequency of mode (0, 2) and then calculate the total impedance Z at three different frequencies near this resonance with $\epsilon_r/\epsilon_o = 4.2$ and $\tan\delta = 0.01$ for the previously described planar structure. The three Z's represent the port impedance of the structure as if measurements had been performed. We then substitute the *measured impedances* into (11) and (13) and calculate the corresponding complex permittivities. To validate this approach, first it is recognized that (1) for the impedance of the structure has already been verified by experimental measurements [16]. Second, since this approach is based on measuring the impedance near a modal resonant frequency, the accuracy of the method must be investigated as a function of the closeness of the measured frequency to the actual modal resonant frequency. In practice, the measurement frequency could differ from the exact resonance due to coarse frequency resolution of the measurement equipment, to an imperfect structure geometry, or to an imprecisely matched coupling between the detector and the generator. To illustrate these points, we summarize the complex permittivity ϵ and $\tan\delta$ calculation results at three frequencies slightly different from the theoretical resonances of the (0, 2) and (2, 2) modes in Tables II and III, respectively, and perform a simple error analysis. The data in these tables show that the error in both ϵ and $\tan\delta$ significantly increases when the offset from the modal resonance becomes large; the error in $\tan\delta$ is more sensitive than that in ϵ especially for a large frequency offset. The error is mainly due to the contribution to the terminal impedance from other nonresonant modes at the selected frequencies.

TABLE IV
DIELECTRIC CONSTANT, LOSS TANGENT, AND THEIR RELATIVE ERRORS CALCULATED FROM MEASURED IMPEDANCE NEAR THE FIRST TWO OBSERVABLE MODAL RESONANCES OF THE PCB

Freq. (GHz)	0.8900	1.2475
Z^r (Ω)	59.20	58.33
Z^i (Ω)	-45.13	27.92
ϵ_r/ϵ_o	4.1995	4.2159
Rel. Error (ϵ_r/ϵ_o) (%)	0.1	0.4
$\tan\delta$	.0115	.0107
Rel. Error ($\tan\delta$) (%)	15	7.0

To further verify the model, and to provide an example of the proposed approach, the S-parameter data for the PCB was measured with a Hewlett-Packard HP-8510C network analyzer. The analyzer frequency was swept across a range of frequencies and the measured S_{11} was converted into impedance. The modal resonant frequencies were estimated as the frequencies at which the resistance peaked and the reactance magnitude was minimum. At the two observed modal resonances, (11) and (13) were used to calculate dielectric constant and loss tangent. Table IV summarizes the complex permittivity calculation results for the two resonant frequencies studied in Tables II and III. These measured relative dielectric constant and loss tangent values in Table IV are near the reported values and the model-predicted values. The error is mainly due to the offset of the measurement frequency from the actual resonant frequency especially for the (0, 2)/(2, 0) modes or due to the contribution to the terminal impedance from other nonresonant modes at the selected frequencies.

IV. ANALYSIS OF ERROR DUE TO FINITELY CONDUCTING PLANES

In the previous discussion, we assumed that the copper planes are perfectly conducting. However, in practice, measurements of loss factors of this structure include losses predominantly due to dielectric and plane conductor resistivity losses [20]. In this case, a perturbation approach can be used to separate the conductor loss from the total measured loss of the structure. Assuming that the electromagnetic fields in the lossy dielectric are not greatly different from the fields of the lossless case, the power loss in the conducting planes and the Q of the structure accounting for the lossy conducting planes can be calculated by a standard technique [21], i.e., the ratio of the $\tan\delta$ of the dielectric to the total loss can be calculated or the $\tan\delta$ can be separated from the total loss. As a first-order approximation, we propose an analytical scheme to evaluate the effect of conductor loss on the calculated total $\tan\delta$. When considering a small dissipation in the structure, the wavenumber k should be formally replaced by

$$k = k' - jk'' \tag{17}$$

with

$$k'' = \frac{\omega}{2}\left(\tan\delta + \frac{r}{d}\right)\sqrt{\mu\epsilon_r} \tag{18}$$

where r is the skin depth of the conductor. This expression for k'' is derived in [17] and illustrates the contribution of the conductor and dielectric losses to the imaginary part of the wavenumber.

To estimate the contribution of conductor and dielectric losses to the total measured $\tan\delta$, we define the total measured $\tan\delta$ as the apparent $\tan\delta_{\text{ap}}$, which includes both conductor and dielectric loss contributions, and express plate-conductivity $\tan\delta_{\text{ap}}$, in terms of the complex wavenumber, the dielectric $\tan\delta$, and the system parameters

$$\tan\delta_{\text{ap}} = \frac{\frac{2k_r k_i}{\mu\omega^2}}{\frac{(k_r^2 - k_i^2)}{\mu\omega^2}} = \frac{\tan\delta + \frac{r}{d}}{1 - .25\left(\tan\delta + \frac{r}{d}\right)^2}. \tag{19}$$

For low-loss materials, $\tan\delta \ll 1$. It is seen that if the ratio $r/d \ll \tan\delta$ then $\tan\delta_{\text{ap}} \simeq \tan\delta$.

In the example presented in Section III for the copper parallel-plate capacitor filled by a 1.524-mm-thick GETEK® dielectric at 1 GHz, $r = 2.1$ μm and $r/d = 1.4 \times 10^{-3}$. The reported $\tan\delta$ around 1 GHz is 0.01. Thus, according to (19), the error in using (13) for calculating $\tan\delta$ is about 14%.

From (19), the upper limit on the error due to the metal resistivity can be estimated as $(r/d)/\tan\delta$, which shows that when $r/d \ll \tan\delta$, the conductor loss insignificantly contributes to the measured loss tangent.

Complex dielectric constants for materials typically used in microwave integrated circuits are usually in the range of 2–20 for ϵ_r and 0.0001–0.1 for $\tan\delta$ [22]. To ignore the conductor loss in the estimated $\tan\delta_{\text{ap}}$ value, the following three conditions must be assured:

1) planes are good conductors;
2) dielectric layer is relatively thick as is reported in [23];
3) measurement frequency is high, such that the conductor loss is much smaller than the dielectric loss.

However, when the dielectric loss is very small, i.e., $\tan\delta \approx 0.0001$, the contribution of the conductor loss in the frequency range of interest is no longer small compared to the dielectric loss. Thus, the apparent $\tan\delta_{\text{ap}}$ values can be significantly different from the $\tan\delta$ of the dielectric, in which case (19) will produce significant errors in $\tan\delta$.

V. CONCLUSION

Our analytical-formula-based approach provides physical and mathematical insight into the relation between complex permittivity and port impedance for dielectric materials between parallel plates. Closed-form full-wave-based analytical expressions were developed for calculating complex permittivity near high-order modal resonant frequencies at which the impedance contributed by the resonant mode dominates the impedance of other modes. These equations enable the calculation of complex permittivity from impedance measurements and structural dimensions for low-loss dielectric materials in electrically wide structures at high frequencies. Based on this theory, computer simulation for complex permittivities at or near several resonant frequencies and the comparison between the measurement data and the model prediction at the first two observable resonances of the PCB capacitor were presented and the preliminary results were analyzed. We found that when the operating frequency of a parallel-plate structure is far below the system resonant frequencies, the static approach based on the use of the measured real and imaginary parts of the input admittance of the structure provides a good estimate of the complex permittivity. However, if the structure is operated at high frequencies, then the high-order-mode approach presented in this paper should be used to obtain the correct value for complex permittivity. In addition, an easily applied analytical expression for estimating the effect of loss in the parallel plates on the calculated complex permittivity was also developed, which links the physical quantity $\tan\delta$ with the engineering design parameters.

To further validate this method, we will make measurements at or near the modal resonances of a parallel-plate structure and perform a detailed comparison and error analysis on this study. For the more general case of obtaining the complex permittivity at arbitrary frequencies, it is necessary to employ the total impedance formula for the structure rather than the individual modal impedances around resonances. The general case can be investigated by numerically solving the inverse problem, which will be a subject for further research.

REFERENCES

[1] G.-T. Lei, R. W. Techentin, and B. K. Gilbert, "Electrical behavior of multichip modules in the presence of power and ground plane noise," in *IEEE Proc. Int. Conf. Multichip Modules*, Denver, CO, Apr. 1995, pp. 175–184.

[2] W. Rueggeberg, "Determination of complex permittivity of arbitrarily dimensioned dielectric modules at microwave frequencies," *IEEE Trans. Microwave Theory Tech.*, vol. MTT-19, pp. 517–521, June 1971.

[3] H. Ermert, "Accurate measurement of complex permittivity of low-loss MIC substrate," *Nachrichtentechn. Z* ., vol. 27, pp. 43–46, 1974.

[4] M. A. Tsankov, "Permittivity measurement of a thin slab centrally located in a rectangular waveguide," *J. Phys. E, Sci. Instrum.*, vol. 8, no. 11, pp. 963–966, 1975.

[5] M. C. Decreton and M. S. Ramachandraiah, "Nondestructive measurement of complex permittivity for dielectric slabs," *IEEE Trans. Microwave Theory Tech.*, vol. MTT-23, pp. 1077–1079, Dec. 1975.

[6] D. Kajfez, W. P. Wheless Jr., and R. T. Ward, "Influence of an airgap on the measurement of dielectric constant by a parallel-plate dielectric resonator," *Proc. Inst. Elect. Eng.*, vol. 133, pt. H, no. 4, pp. 253–258, Aug. 1986.

[7] J. Baker-Jarvis, R. G. Geyer, and P. D. Domich, "A nonlinear least-squares solution with causality constraints applied to transmission line permittivity and permeability determination," *IEEE Trans. Instrum. Meas.*, vol. 41, pp. 646–652, Oct. 1992.

[8] G. K. Gopalakrishnan and K. Chang, "Study of slits in microstrip ring resonators for microwave and optoelectronic applications," *Microwave Opt. Technol. Lett.*, vol. 5, no. 2, pp. 76–78, Feb. 1992.

[9] Y. Kobayashi and T. Senju, "Resonant modes in shielded uniaxial-anisotropic dielectric rod resonators," *IEEE Trans. Microwave Theory Tech.*, vol. 41, pp. 2198–2205, Dec. 1993.

[10] J. Abdulnour, C. Akyel, and K. Wu, "A generic approach for permittivity measurement of dielectric materials using a discontinuity in a rectangular waveguide or a microstrip line," *IEEE Trans. Microwave Theory Tech.*, vol. 43, pp. 1060–1066, May 1995.

[11] S. Vasudevan and A. Shaikh, "Microwave characterization of low temperature cofired ceramic tape," in *Proc. Int. Conf. Multichip Modules*, Denver, CO, Apr. 1995, pp. 164–174.

[12] P. K. Singh *et al.*, "High frequency measurement of dielectric thin films," in *IEEE MTT-S Int. Microwave Symp. Dig.*, San Diego, CA, May 1994, pp. 1457–1460.

[13] W. Williamson III *et al.*, "High frequency dielectric properties of thin-film PZT capacitors," *Integrated Ferroelectronics*, vol. 10, pp. 335–342, 1995.

[14] R. F. Harrington, *Time-Harmonic Electromagnetic Fields*. New York: McGraw-Hill, 1961, ch. 1.

[15] J. D. Jackson, *Classical Electrodynamics*. New York: Wiley, 1975, ch. 6.

[16] G.-T. Lei *et al.*, "Wave model solution to the ground/power plane noise problem," *IEEE Trans. Instrum. Meas.*, vol. 44, pp. 300–303, Apr. 1995.

[17] T. Okoshi, *Planar Circuits for Microwaves and Lightwaves*. Berlin, Germany: Springer-Verlag, 1985.

[18] L. D. Landau and E. M. Lifshitz, *Electrodynamics of Continuous Media*. Reading, MA: Addison-Wesley, 1960, ch. 11.

[19] S. Ramo, J. R. Whinnery, and T. V. Duzer, *Fields and Waves in Communication Electronics*. New York: Wiley, 1967, ch. 6, 11.

[20] T. Edwards, *Foundation for Microstrip Circuit Design*, 2nd ed. New York: Wiley, 1992.

[21] D. M. Pozar, *Microwave Engineering*. Reading, MA: Addison-Wesley, 1990, ch. 7.

[22] R. K. Hoffmann, *Handbook of Microwave Integrated Circuits*. Norwood, MA: Artech House, 1987.

[23] J. Fang *et al.*, "Effect of losses in power and ground planes in the simulation of simultaneous switching noise," in *IEEE Topical Meeting Elect. Performance Electron. Packaging*, Monterey, CA, 1994, pp. 110–112.

Robert H. Voelker (S'81–M'90–SM'95) was born in Midland, MI. He received the B.S.E. *summa cum laude*, M.S.E., and Ph.D. degrees in electrical engineering from the University of Michigan at Ann Arbor, in 1982, 1983, and 1989, respectively.

In the 1980's, he pioneered an original approach to the rigorous and comprehensive time-domain modeling of nonlinear high-speed digital and microwave circuits. This technique is based on incorporating three-terminal semiconductor device circuit models in a time-domain finite-difference-type full-wave electromagnetic field simulator. He is currently a Technical Staff Member in the Sun Microelectronics Division of Sun Microsystems, Inc., Palo Alto, CA, where he investigates signal integrity issues in high-speed digital integrated circuits.

Dr. Voelker is a member of Tau Beta Pi and Eta Kappa Nu. He was an IBM Graduate Fellow (1983–1984) and a Shell Doctoral Fellow (1984–1987), and has held a U.S. Army Research Office Fellowship (1987–1989).

Guang-Tsai Lei (M'97) received the M.S. degree in physics from the University of Notre Dame, Notre Dame, IN, in 1984, and the M.E. degree in electrical engineering from the University of Kansas (KU), Lawrence, in 1987.

In 1987, she gained a full-time research position at the Mayo Clinic in Rochester, MN, as an Engineer/Systems Analyst. In 1990, she joined the Special Purpose Processor Development Group, Mayo Foundation, Rochester, MN. Her assignments in this group included the development of the thermomechanical and electrical modeling and simulation techniques for integrated circuits and MCM's using her experience with numerical techniques. More recently, she has been employing her extensive electrical engineering and mathematical background in the development of new methods for the modeling and simulation of the electromagnetic environment of GaAs integrated circuits, PCB's, and MCM's operating at high system clock rates and wide signal bandwidths.

Ms. Lei is a member of Tau Beta Pi.

Guang-Wen Pan (S'81–M'84–SM'94), for a photograph and biography, see this issue, p. 1835.

Barry K. Gilbert (S'62–M'70–SM'87), for a photograph and biography, see this issue, p. 1835.